
This is an electronic reprint of the original article.
This reprint may differ from the original in pagination and typographic detail.

Laakso, Mikko; Rajamäki, Robin; Wichman, Risto; Koivunen, Visa
Phase-coherent multichannel SDR - Sparse array beamforming

Published in:
28th European Signal Processing Conference, EUSIPCO 2020 - Proceedings

DOI:
[10.23919/Eusipco47968.2020.9287664](https://doi.org/10.23919/Eusipco47968.2020.9287664)

Published: 01/01/2020

Document Version
Publisher's PDF, also known as Version of record

Please cite the original version:
Laakso, M., Rajamäki, R., Wichman, R., & Koivunen, V. (2020). Phase-coherent multichannel SDR - Sparse array beamforming. In *28th European Signal Processing Conference, EUSIPCO 2020 - Proceedings* (pp. 1856-1860). Article 9287664 (European Signal Processing Conference). European Association For Signal and Image Processing. <https://doi.org/10.23919/Eusipco47968.2020.9287664>

This material is protected by copyright and other intellectual property rights, and duplication or sale of all or part of any of the repository collections is not permitted, except that material may be duplicated by you for your research use or educational purposes in electronic or print form. You must obtain permission for any other use. Electronic or print copies may not be offered, whether for sale or otherwise to anyone who is not an authorised user.

Phase-coherent multichannel SDR - Sparse array beamforming

Mikko Laakso, Robin Rajamäki, Risto Wichman, Visa Koivunen
Department of Signal Processing and Acoustics
Aalto University
Espoo, Finland
mikko.t.laakso@aalto.fi, *firstname.lastname@aalto.fi*

Abstract—We introduce a modular and affordable coherent multichannel software-defined radio (SDR) receiver and demonstrate its performance by direction-of-arrival (DOA) estimation on signals collected from a 7 X 3 element uniform rectangular array antenna, comparing the results between the full and sparse arrays. Sparse sensor arrays can reach the resolution of a fully populated array with reduced number of elements, which relaxes the required structural complexity of e.g. antenna arrays. Moreover, sparse arrays facilitate significant cost reduction since fewer expensive RF-IF front ends are needed. Results from the collected data set are analyzed with Multiple Signal Classification (MUSIC) DOA estimator. Generally, the sparse array estimates agree with the full array.

Index Terms—sparse array, coherent receiver, DOA estimation

I. INTRODUCTION

Phase-coherent multichannel transceivers based on commercial software-defined radios (SDR) are often prohibitively expensive for low-budget research and prototyping. A prime example of such a system is the Lund University Massive MIMO testbed [1]. Owing to this, affordability was the main motivation for designing a multichannel platform based on the inexpensive and easily obtainable RTL-SDR receiver. The proposed expandable system is able to operate on host computers with limited computing resources and transfer the sample data over a network to MATLAB for processing. The RTL-SDR, originally a USB DVB-T tuner, supports sample rates up to 2.56 MHz and gives access to a stream of 8-bit in-phase and quadrature samples. Compared to the Ettus Research USRP radios used in [1], the RTL-SDR bandwidth is modest and the system does not have transmit capability. On the other hand, the cost per channel with RTL-SDR is a fraction of that compared to USRP or WARP [2] platforms. A brief description of the developed coherent system is given in the next section, and for more information, see [3].

The developed multichannel receiver makes it possible to verify multiantenna algorithms with a large number of receiver chains beyond 1 – 4 antennas typically available with commercial SDRs. In this paper, sparse array processing is applied on signals received with the coherent RTL-SDR receiver connected to a uniform rectangular array (URA) antenna. Sparse array configuration is obtained in this study by deactivating certain redundant physical elements in the array

such that a virtual array called co-array remains uniformly spaced. The goal is to demonstrate the performance of the sparse array processing on real signals and hardware instead of simulations.

In addition to radio frequency (RF) applications, direction-of-arrival (DOA) estimation methods find use in various other sensing modalities. The field of sensor array signal processing has developed various accurate methods to estimate signal emitter direction. However, the resolution of the DOA estimate and the number of simultaneous sources a given method can resolve depend on the number of sensors in the array. Sparse arrays avoid the increasing hardware complexity and cost in large sensor arrays by exploiting spatial redundancy of the array geometry. Depending on the sparse geometry, the increased distance between adjacent sensors can also help mitigate the problem of mutual coupling between array elements [4], [5].

This paper is organized as follows: section II introduces the coherent multichannel software-defined radio (SDR) receiver. Section III provides brief explanation of sparse arrays and sparse array processing. In section IV, the signal model is defined and the DOA estimation method described. These are followed by measurements and results in section V and finally conclusion in section VI.

II. PHASE-COHERENT MULTICHANNEL SDR RECEIVER

The RTL-SDR is a low-IF (intermediate frequency) architecture, consisting of the RTL2832U demodulator and a Rafael Micro R820T/2 tuner. While the device is produced with various tuners by different manufacturers, all commonly referred to as RTL-SDR, the design proposed here only functions with R820T/2 tuner models. This is because R820T/2 tuner allows to disable frequency synthesis dithering, which is crucial for phase coherent operation.

As already stated, the coherent receiver is based on the array of RTL-SDR receivers that are originally separate dongles. The receivers in the system are modified to be driven by a common clock signal and connected to a switchable reference noise generator, as visualized in Fig. 1. The signal receivers are housed in a coupler module, built on top of an USB hub, which accommodates 7 RTL-SDR receivers. To give an idea of the price range, excluding assembling, the hardware costs for a

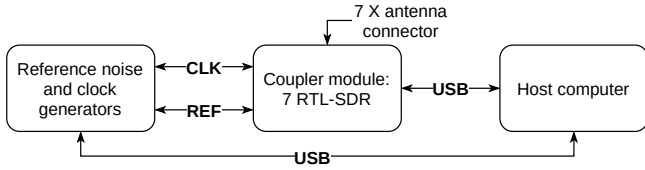


Fig. 1: Block diagram of a receiver system with one coupler module.

7-receiver coupler module are approximately 150€. Thus far, five of such coupler modules have been tested simultaneously, adding to a total of 35 signal channels. Assembling one module by a capable person takes roughly two days. To the best of our knowledge, this is the most economical solution for a massive multichannel SDR receiver available.

A dedicated reference receiver records only the reference noise, sample vector \mathbf{r} , which is generated with a reverse-biased Zener-diode. The same noise is distributed to the signal receivers with directional couplers on the antenna lines of the custom-built coupler circuit board. This enables aligning the signal sample streams in time and phase with cross-correlation. We simply find the maximum of the cross-correlation estimate $|\hat{\phi}_{\mathbf{x}_n \mathbf{r}}(l)|$ for each signal vector \mathbf{x} . To limit the computational load on the host computer doing the processing, shifting the signal stream timing is performed by adjusting the RTL-SDR hardware resampler, originally intended to correct carrier frequency offsets. To further reduce the processing load, the calculation of the correlation is switched off once a given signal channel is deemed time synchronized. Software which automates the described synchronization process, including a client for MATLAB, is written in C++ and published under GPLv3.

As opposed to the sampling clock which all the receivers obtain from a common source in Fig 1, the tuner RF oscillator is derived from this common clock via phase-locked loop (PLL) frequency synthesis. The PLL acquires lock in an arbitrary phase, and therefore the phase needs to be calibrated whenever the receiver is retuned. It was also observed that the relative phases of the signal streams drift slowly during the operation. Fortunately, the rate of this drift is typically less than 1° per minute. Therefore, before each measurement, we calculate a phase-correction coefficient α_n for all signal channels 1 to n with $\alpha_n = \langle \mathbf{x}_n^*, \mathbf{r} \rangle / |\langle \mathbf{x}_n^*, \mathbf{r} \rangle|$. Coefficient α_n is averaged over a few frames to reduce noise and then the corrected receiver phase is assumed coherent for the duration of the measurement. The reference noise is enabled only during the time synchronization and calculation of the phasors α , otherwise it dramatically degrades signal-to-noise ratio (SNR). Furthermore, the noise is by design highly correlated and relatively strong across the signal channels, which is problematic for DOA techniques. If it is not switched off, DOA estimation techniques will show a strong signal impinging from 0° , directly towards the broadside of the antenna.

III. SPARSE ARRAYS

This section introduces the key concepts of sparse arrays and signal processing for sparse arrays. A sparse sensor array achieves the same aperture as a full array using a reduced number of physical elements. Only a brief description of the co-array concept is given below for the one dimensional case. For more information, refer to, for instance [6] and [7].

A. Difference co-array

The *sparse array* is typically approached through a virtual co-array of element sums or differences. The difference co-array method is well-suited to passive sensing applications, whereas the sum co-array is typically used for active sensing [5]. In most cases, the physical distance between the array elements is half wavelength, $\lambda/2$, and the array is hereafter described in integer d multiples of this distance. Consider a contiguous linear array with N equispaced elements, with an aperture of $L = N - 1$. Let $\mathcal{D} = \{0, 1, \dots, N - 1\}$ be the set of normalized element distances, $|\mathcal{D}| = N$, then the difference co-array \mathcal{D}_Δ is [6]:

$$\mathcal{D}_\Delta = \{d_j - d_k \mid d \in \mathcal{D}\} \quad j, k = 0, 1, \dots, N - 1. \quad (1)$$

With increasing N , the redundancy in (1) increases, i.e. $d_j - d_k$ above yield multiple identical differences. A fully populated linear array with $N \geq 3$ always has a redundant co-array.

When the physical array is sparse, \mathcal{D} is not a contiguous set of integers and the array is said to contain holes. Certain geometries can still represent the contiguous set of integers $\{0, 1, \dots, L\}$ with the co-array (1). However, it is known that any sparse array with $N > 4$ has a redundant co-array [8]. A Minimum-redundancy array (MRA) [9] minimizes $|\mathcal{D}|$ such that $\mathcal{D}_\Delta = \{0, 1, \dots, L\}$, that is, finds an array geometry with the smallest number of elements that can still produce a uniform co-array. Fig. 2 shows an example of an MRA with $N = 4$ and a uniform linear array (ULA) with $N = 7$

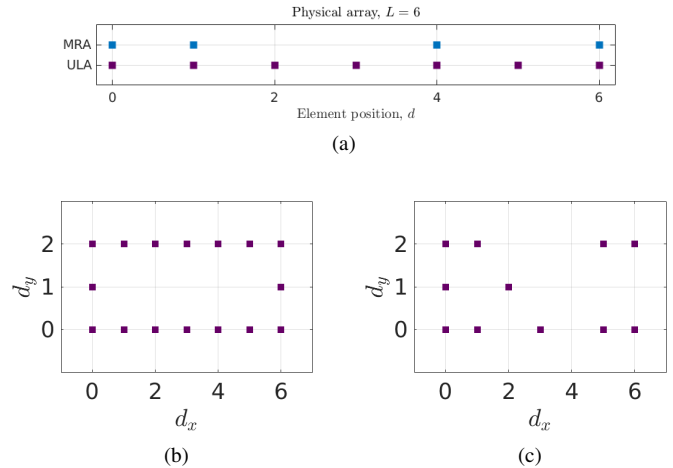


Fig. 2: Array configurations: top 4-element linear MRA, bottom left Boundary Array, bottom right arbitrary 11 element array with equal co-array

elements. The two arrays achieve the same aperture $L = 6$ without loss in the number of sources one can resolve. A sparse ruler analogy is often used in explaining the sparse array, and turns out this problem is closely related to the concept of Golomb rulers researched in the field of number theory, also discussed in [8]. A closed-form solution for finding minimum-redundancy array geometries is not known and the search for such optimal geometries for large N is a computationally hard combinatorial problem [5].

Naturally, the co-array approach can be extended to planar arrays, depicted in Fig. 2. In a Boundary Array, the sensors elements are placed on a convex boundary, which ensures a fully populated co-array [10]. Also shown is an arbitrary rectangular N -element array, which has the same co-array support as the full array, found with an exhaustive search. Note that both of the depicted reduced array geometries have the same aperture as the full 7×3 URA.

B. Co-array processing

For eigenspace methods such as MUSIC, which operate on the estimated signal covariance matrices, the $\mathbb{C}^{(L+1) \times (L+1)}$ matrix \mathbf{R}_A can be directly expanded from the estimated $\mathbb{C}^{N \times N}$ sparse array covariance matrix. One such method is *covariance matrix augmentation* (CMA), introduced by Pillai et al. in [11]. CMA imposes a Toeplitz structure and imputes the missing spatial correlations using the corresponding lags from \mathcal{D}_Δ . Averaging can be employed for redundant lags. The augmented covariance becomes

$$[\mathbf{R}_A]_{q,r} = \frac{\sum_{n,m} \mathbb{1}(d_{\Delta, N_\Delta+q-r} = d_n - d_m) [\mathbf{R}_{\mathbf{xx}}]_{n,m}}{v_\Delta(d_{\Delta, N_\Delta+q-r})} \quad (2)$$

where $v_\Delta(d_\Delta) = \sum_{n,m} \mathbb{1}(d_\Delta = d_n - d_m)$ is the co-array multiplicity function, $\mathbb{1}(\cdot)$ is an indicator function, $N_\Delta = (|\mathcal{D}_\Delta| + 1)/2$ and $d_{\Delta,i}$ denotes the i th difference co-array element (ordered in ascending order), with $i = 1, 2, \dots, |\mathcal{D}_\Delta|$. However, the resulting augmented $\mathbf{R}_{\mathbf{xx}}$ is not anymore guaranteed to be positive definite [12]. This has implications in scenarios where e.g. the number of signal sources is not known a priori and is to be estimated from eigenvalue magnitudes. Co-array based DOA has also been experimentally verified to be sensitive to multipath propagation [13].

IV. DIRECTION FINDING

Assuming a signal impinging on the array from a far-field source, the signal model reads

$$\mathbf{x}(t) = \mathbf{a}s(t) + \mathbf{n}(t) \quad (3)$$

where $\mathbf{x}(t)$ is the received signal, $s(t)$ is the transmitted signal vector, \mathbf{a} the array steering vector and $\mathbf{n}(t)$ represents the i.i.d gaussian noise. We use the well-known MUSIC algorithm for DOA estimation, for which the spatial spectrum power as a function of source azimuth angle α and elevation β reads

$$P_{MUSIC}(\alpha, \beta) = \frac{1}{\|\mathbf{Q}_n^\dagger \mathbf{a}(\alpha, \beta)\|^2} \quad (4)$$

where \dagger denotes the Hermitian transpose and \mathbf{Q}_n is the noise subspace, orthogonal to all the signals obtained from the full

eigenvalue decomposition of the covariance matrix, i.e. $\mathbf{R}_{\mathbf{xx}} = \mathbf{Q}_s \Lambda_s \mathbf{Q}_s^\dagger + \mathbf{Q}_n \Lambda_n \mathbf{Q}_n^\dagger$ [14]. The steering vector for azimuth α and elevation β can be expressed as

$$\mathbf{a}(\alpha, \beta) = \mathbf{a}_y(\alpha, \beta) \otimes \mathbf{a}_x(\alpha, \beta)$$

where \otimes is the Kronecker product and the horizontal and vertical components are

$$\begin{aligned} \mathbf{a}_x(\alpha, \beta) &= [1 \quad e^{jkd \cos \beta \cos \alpha} \quad \dots \quad e^{jkd(M_x-1) \cos \beta \cos \alpha}]^T \\ \mathbf{a}_y(\alpha, \beta) &= [1 \quad e^{jkd \cos \beta \sin \alpha} \quad \dots \quad e^{jkd(M_y-1) \cos \beta \sin \alpha}]^T \end{aligned}$$

Producing the spatial spectrum is computationally expensive, as (4) is evaluated on a 2D grid of (α, β) [15]. Methods have been developed to relax the computational demand, but this is out of the scope of this paper.

V. MEASUREMENTS AND RESULTS

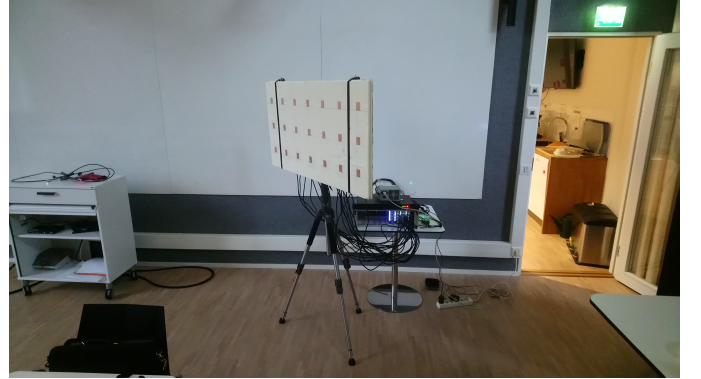


Fig. 3: Measurement setup

A uniform rectangular array (URA) patch antenna, seen in Fig. 3, with 7×3 elements was constructed for the measurements. To reduce the physical size of the elements, the patches were designed with planar inverted-F (PIFA) geometry [16], intended to operate on the license-free 868 MHz ISM band. The antenna was constructed from a polyurethane insulation board acting as the dielectric material, with thin copper patches as the actual PIFA elements. As a result, the array is lightweight, inexpensive, easy to carry and assemble. The elements are thus placed on a rectangular $\lambda/2$ grid, which for the purposes of this research, is assumed ideal.

A series of measurements was conducted in a lecture hall, recording the received data for each true transmitter position. Naturally, the environment is reflective so that the resulting DOA estimates will be hampered by interfering echoes. More accurate results could be obtained in a controlled testing environment, but in the spirit of affordable research and quick prototyping and testing, we chose not to make the measurements in an anechoic chamber. The transmitting SDR was broadcasting a randomized QPSK signal and to ensure far-field conditions, the transmitting SDR was at a distance greater than the Fraunhofer distance. The Fraunhofer distance, defined from the aperture $d_F = L^2 \lambda / 2$ for the antenna array,

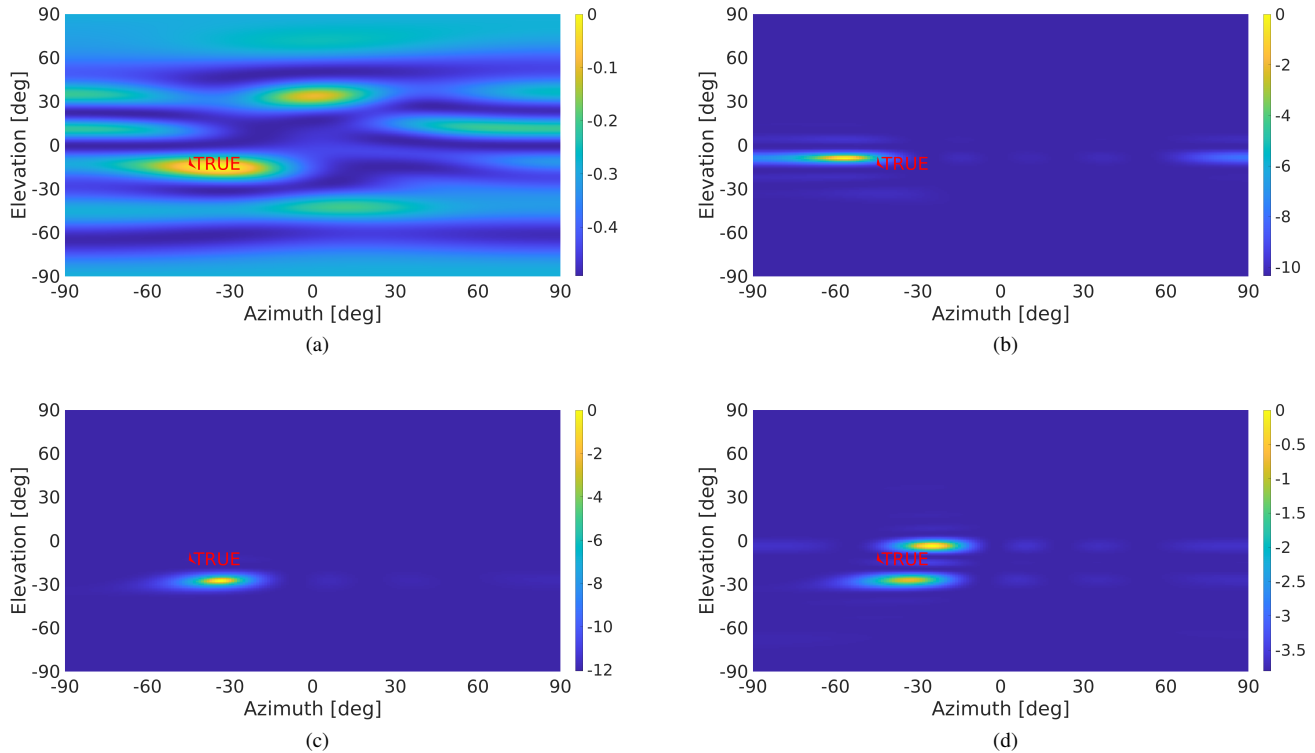


Fig. 4: MUSIC pseudospectra using: a) full 7 x 3 array without co-array processing, b) CMA on full 7 x 3 array, c) 16 element Boundary Array with CMA, d) 11 element arbitrary array with CMA

is approximately 6 meters on the horizontal plane and much less on the vertical plane, since $L_x = 6$ and $L_y = 2$.

Altogether, 13 frames of 81920 samples were collected and for each frame, 8192 snapshots were used in estimating the signal covariance matrix. In most of the collected frames, the DOA estimate tracks the signal source correctly. The spatial spectra in Fig. 4, except top left, were computed with covariance matrix augmentation. Furthermore, the fully populated and thinned arrays from Fig. 2, have the same co-array \mathcal{D}_Δ . The thinned arrays yield an estimate in the same general direction, but some deviation is seen between the two reduced antenna geometries. This deviation could be accounted to be the effect of coherent reflections. Clearly, the co-array processing extends the dynamic range considerably and furthermore, can be used to enhance the performance of the existing full array.

VI. CONCLUSION

We demonstrated the performance of an affordable custom-built multiantenna receiver, based on RTL-SDR dongles, by direction-of-arrival (DOA) estimation using sparse antenna arrays. Evidently, the multiple receiver chains achieve phase-coherence since the DOA estimates are reasonable. Furthermore, the estimates from the sparse array with fewer physical elements agree with the full array. The difference co-array approach is a straightforward, yet sophisticated approach for

sparse array processing, but it is not suitable as such to e.g. transmit beamforming.

One interesting topic for further work is to utilize multiple signal sources on the move. One example of a real-world moving signal source would be the 868 MHz FLARM (flight and alarm) transponder system aboard glider aircraft and glider tow planes. The FLARM collision warning signal encodes the aircraft GPS coordinates and altitude reading, which could be decoded to estimate the true DOA in such scenario.

Finally, the source code and description of supporting hardware for the multichannel receiver are available in the Git repository <https://github.com/mlaaks/coherent-rtlsdr>.

REFERENCES

- [1] S. Malkowsky et al., "The World's First Real-Time Testbed for Massive MIMO: Design, Implementation and Validation," in *IEEE Access*, vol. 5, pp. 9073-9088, 2017.
- [2] P. Murphy, A. Sabharwal and B. Aazhang, "Design of WARP: A wireless open-access research platform," *2006 14th European Signal Processing Conference*, Florence, 2006, pp. 1-5.
- [3] M. Laakso, "Multichannel coherent receiver on the RTL-SDR," M.Sc. Thesis, Sch. of Electrical Engineering, Aalto Univ., Espoo, 2019. Available: <https://aaltodoc.aalto.fi/handle/123456789/37163>
- [4] C. Liu and P. P. Vaidyanathan, "Super Nested Arrays: Linear Sparse Arrays With Reduced Mutual Coupling—Part I: Fundamentals," in *IEEE Transactions on Signal Processing*, vol. 64, no. 15, pp. 3997-4012, 1 Aug. 2016.
- [5] R. Rajamäki and V. Koivunen, "Comparison of Sparse Sensor Array Configurations with Constrained Aperture for Passive Sensing," *2017 IEEE Radar Conference (RadarConf)*, Seattle, WA, 2017, pp. 0797-0802.

- [6] R. T. Hoor and S. A. Kassam, "The unifying role of the coarray in aperture synthesis for coherent and incoherent imaging," in *Proceedings of the IEEE*, vol. 78, no. 4, pp. 735-752, April 1990.
- [7] P. Pal and P. P. Vaidyanathan, "Nested Arrays: A Novel Approach to Array Processing With Enhanced Degrees of Freedom," in *IEEE Transactions on Signal Processing*, vol. 58, no. 8, pp. 4167-4181, Aug. 2010.
- [8] D. A. Linebarger, I. H. Sudborough and I. G. Tollis, "Difference bases and sparse sensor arrays," *IEEE Transactions on Information Theory*, vol. 39, no. 2, pp. 716-721, Mar. 1993.
- [9] A. Moffet, "Minimum-redundancy linear arrays," in *IEEE Transactions on Antennas and Propagation*, vol. 16, no. 2, pp. 172-175, March 1968.
- [10] R. Rajamäki and V. Koivunen, "Sparse Active Rectangular Array with Few Closely Spaced Elements," *IEEE Signal Processing Letters*, 25(12) pp. 1820-1824, 2018.
- [11] S. Pillai, F. Haber and Y. Bar-Ness, "A new approach to array geometry for improved spatial spectrum estimation," *ICASSP '85. IEEE International Conference on Acoustics, Speech, and Signal Processing*, Tampa, FL, USA, 1985, pp. 1816-1819.
- [12] Y. I. Abramovich, D. A. Gray, A. Y. Gorokhov and N. K. Spencer, "Positive-definite Toeplitz completion in DOA estimation for nonuniform linear antenna arrays. I. Fully augmentable arrays," *IEEE Transactions on Signal Processing*, vol. 46, no. 9, pp. 2458-2471, Sept. 1998.
- [13] J. Wang, H. Xu, G. J. T. Leus and G. A. E. Vandenbosch, "Experimental Assessment of the Coarray Concept for DoA Estimation in Wireless Communications," *IEEE Transactions on Antennas and Propagation*, vol. 66, no. 6, pp. 3064-3075, June 2018.
- [14] R. Schmidt, "Multiple emitter location and signal parameter estimation," *IEEE Transactions on Antennas and Propagation*, vol.34, no.3, pp.276-280, Mar. 1986.
- [15] X. He Z. Zhang and W. Wang, "DOA estimation with uniform rectangular array in the presence of mutual coupling," *2016 2nd IEEE International Conference on Computer and Communications (ICCC)*, Chengdu, 2016, pp. 1854-1859.
- [16] C. Balanis, *Antenna Theory - Analysis and Design*. John Wiley & Sons, 2016, pp. 838-840.